

Video Article

Applications of *In Vivo* Functional Testing of the Rat Tibialis Anterior for Evaluating Tissue Engineered Skeletal Muscle Repair

Ellen L. Mintz¹, Juliana A. Passipieri², Daniel Y. Lovell², George J. Christ^{2,3}¹Department of Pathology, University of Virginia²Department of Biomedical Engineering, University of Virginia³Department of Orthopaedic Surgery, University of VirginiaCorrespondence to: George J. Christ at gjc8w@virginia.eduURL: <https://www.jove.com/video/54487>DOI: [doi:10.3791/54487](https://doi.org/10.3791/54487)Keywords: Bioengineering, Issue 116, *In vivo*, muscle force production, peroneal nerve stimulation, tibialis anterior, dorsiflexion, tissue engineering, regenerative medicine, skeletal muscle regeneration, volumetric muscle loss, muscle disease, pathology

Date Published: 10/7/2016

Citation: Mintz, E.L., Passipieri, J.A., Lovell, D.Y., Christ, G.J. Applications of *In Vivo* Functional Testing of the Rat Tibialis Anterior for Evaluating Tissue Engineered Skeletal Muscle Repair. *J. Vis. Exp.* (116), e54487, doi:10.3791/54487 (2016).

Abstract

Despite the regenerative capacity of skeletal muscle, permanent functional and/or cosmetic deficits (e.g., volumetric muscle loss (VML) resulting from traumatic injury, disease and various congenital, genetic and acquired conditions are quite common. Tissue engineering and regenerative medicine technologies have enormous potential to provide a therapeutic solution. However, utilization of biologically relevant animal models in combination with longitudinal assessments of pertinent functional measures are critical to the development of improved regenerative therapeutics for treatment of VML-like injuries. In that regard, a commercial muscle lever system can be used to measure length, tension, force and velocity parameters in skeletal muscle. We used this system, in conjunction with a high power, bi-phase stimulator, to measure *in vivo* force production in response to activation of the anterior crural compartment of the rat hindlimb. We have previously used this equipment to assess the functional impact of VML injury on the tibialis anterior (TA) muscle, as well as the extent of functional recovery following treatment of the injured TA muscle with our tissue engineered muscle repair (TEMR) technology. For such studies, the left foot of an anesthetized rat is securely anchored to a footplate linked to a servomotor, and the common peroneal nerve is stimulated by two percutaneous needle electrodes to elicit muscle contraction and dorsiflexion of the foot. The peroneal nerve stimulation-induced muscle contraction is measured over a range of stimulation frequencies (1-200 Hz), to ensure an eventual plateau in force production that allows for an accurate determination of peak tetanic force. In addition to evaluation of the extent of VML injury as well as the degree of functional recovery following treatment, this methodology can be easily applied to study diverse aspects of muscle physiology and pathophysiology. Such an approach should assist with the more rational development of improved therapeutics for muscle repair and regeneration.

Video Link

The video component of this article can be found at <https://www.jove.com/video/54487/>

Introduction

Skeletal muscle has a remarkable intrinsic capacity for repair in response to injury or disease^{1,2}. Experimentally, the robustness of this regenerative response has been well documented in animal models by studying, for example, the time course of skeletal muscle damage, repair and regeneration after application of myotoxins (e.g., cardiotoxin)³⁻⁷. More specifically, following extensive cardiotoxin-induced muscle damage (38-67% of muscle fibers⁸), regeneration is mediated by satellite cells, the resident stem cells that mature to ultimately become functional muscle fibers^{4,9-13}. The end result is increased post-damage functional regeneration of healthy, force-producing muscle tissue¹⁴⁻¹⁶. Although the details are well beyond the scope of this report, the mechanistic basis for muscle regeneration reflects the carefully orchestrated events of numerous cell types from multiple lineages utilizing canonical signaling pathways critical to both tissue development and morphogenesis^{5,17-21}. Importantly, myotoxin-induced regeneration is enabled by the fact that the extracellular matrix, neuronal innervation and blood vessel perfusion remain structurally intact following cardiotoxin-induced muscle damage^{3,8,22}. In stark contrast, these key tissue structures and components are, by definition, entirely absent in the context of VML injury; where frank loss of tissue, due to a variety of causes, results in permanent functional and cosmetic deficits²³⁻²⁵.

Regardless of the additional challenges associated with muscle repair and regeneration following VML injury in comparison with myotoxin-induced muscle damage, improved understanding of the mechanistic basis for skeletal muscle regeneration and repair, in a variety of contexts, would be well served by utilization of biologically relevant animal models in combination with longitudinal assessments of pertinent functional measures. As discussed herein, studies of the rat hindlimb provide an excellent model system to this end. More specifically, the muscles of the anterior crural compartment (tibialis anterior, extensor digitorum longus (EDL) and hallicus longus (HL)), which are responsible for dorsiflexion of the foot, are easily identified and manipulated. Moreover, they are served by major blood vessels (iliac and branches), and are innervated by nerves (sciatic and branches, including peroneal) running the length of the leg²⁶⁻²⁸. As such, one can use the rat hindlimb model to directly assess skeletal muscle function/pathology *in vivo*, or to evaluate the more indirect impact of pathology-related alterations in blood vessels

or nerves on corresponding skeletal muscle function. In either scenario, the severity of disease, as well as the efficacy of treatment can be determined as a function of muscle force production (torque) and corresponding foot movement²⁹⁻³⁴.

Ideally, force measurements are accompanied by histological studies and gene expression analyses to more rigorously evaluate the structural and molecular status of skeletal muscle. Basic histology and immunohistochemistry, for example, are able to answer questions about muscle size, muscle fiber alignment, extracellular matrix composition, location of nuclei, cell number, and protein localization. Gene expression analysis, in turn, is necessary for identifying the molecular mechanisms that may influence/modulate the maturity of the muscle fibers, disease states, and metabolic activity. While these methods provide crucial information, they generally represent terminal endpoints, and most importantly, they fail to directly address the functional capacity of skeletal muscle, and thus, are correlative rather than causative. However, when histological studies and gene expression analyses are evaluated in conjunction with functional measures, then, mechanisms of force production and functional regeneration can be most accurately identified.

In this regard, the force producing abilities of a muscle can be measured *in vitro*, *in situ*, or *in vivo*. All three approaches have both advantages and limitations. In an *in vitro* experiment, for example, the muscle is completely isolated and removed from the body of the animal. By removing the influences of the blood vessels and nerves that supply the muscle, the contractile ability of the tissue can be determined in a tightly controlled external environment³⁵. *In situ* muscle testing allows the muscle to be isolated, as with *in vitro* preparations, however, the innervation and blood supply remain intact. The benefit of the *in situ* experimental model is that it allows an individual muscle to be studied while the innervation and blood supply is minimally perturbed³⁶. In both *in vitro* and *in situ* experiments, pharmacological treatments may be applied more directly without having to account for the effects of any surrounding tissues or the impact of the circulatory system on the measured contractile responses³⁷. However, *in vivo* function testing, as described herein, is the least invasive technique for evaluating muscle function in its native environment³⁸, and can be performed repeatedly over time (*i.e.*, longitudinally). As such, it will be the focal point of the discussion below.

In this regard, percutaneous electrodes inserted near the muscle of interest, or the motor nerve that serves it, provide an electrical signal to the muscle. A transducer then measures the resultant length or force changes in the activated muscle as directed by a predetermined, customized software protocol. From these data, the physical properties of the muscle can be determined. These include force-frequency, maximal tetanus, force-velocity, stiffness, length tension, and fatigue. Muscle length or force may also be held constant so that the muscle contracts isometrically or isotonicly. Importantly, these experimental protocols can be rapidly performed, easily repeated, and customized- all while the animal is anaesthetized and with a recovery period of hours to days. A single animal can undergo *in vivo* force testing multiple times, thus enabling longitudinal studies of disease models or evaluation of therapeutic platforms/technologies.

As described herein, a commercial muscle lever system in conjunction with a high power, bi-phase stimulator is used to perform *in vivo* muscle function testing to evaluate the contribution of the tibialis anterior muscle of the rat hindlimb to dorsiflexion of the foot via stimulation of the peroneal nerve. We have developed a protocol that is specifically designed to evaluate regenerative medicine/tissue engineering technologies for muscle repair following traumatic VML injury of the rat TA muscle. It should be noted; the EDL and HL need to be dissected out of the anterior crural compartment in order to specifically evaluate the TA muscle (they account for approximately 15-20% of the total tibialis anterior torque measured following peroneal nerve stimulation (Corona *et al.*, 2013)). Because this approach provides comprehensive longitudinal analysis of muscle physiology/function, it can shed important mechanistic insight on numerous other types of physiological investigations as well as a variety of disease or therapeutic areas³⁹. For example, *in vivo* muscle function testing is applicable to studies of exercise physiology, ischemia/reperfusion research, myopathy, nerve damage/neuropathy and vasculopathy, sarcopenia, and muscular dystrophies⁴⁰.

Protocol

All animals were humanely treated and all protocols were approved by the University of Virginia IACUC.

1. Equipment Preparation

1. Ensure that all machines are properly connected.
2. Turn on the computer, followed by the high-power bi-phase stimulator and dual-mode lever system.
3. At this time, place the animal into the anesthesia chamber supplied with 2% isoflurane, and turn on the heating element so that the platform is heated to 37 °C.
4. Place the electrodes in 70% ethanol so that the polytetrafluoroethylene (PTFE) coated tips are submerged and will be disinfected while setting up the device and software.
5. Locate and open the lever system control software on the desktop.
NOTE: This will be the software needed to perform functional testing.

2. Software Setup

1. Once the program is opened (**Figure 1A**), change the parameters for Instant Stim under the Setup menu to the desired values.
NOTE: In this protocol, all parameters remain at the preset levels with the exception of "Run Time (s)", which is changed to 180 sec (**Figure 1B**).
2. Create an Autosave folder under the Setup menu.
3. Locate a type-able window labeled "Autosave Base". Input the name of the sample, for example "Rat1-date-timepoint". Directly to the left of the "Autosave Base" type-able window, click on the box to "Enable Autosave."
4. At the top of the Control Screen, select "Sequencer". A new window will open. On the bottom of the new window, select "Open Sequence". A new window will open. Select the premade sequence and click OK. A protocol list with sequence parameters including frequency, duration of stimuli, and rest time will develop in the window named: Sequence Editor (**Figure 1C**). Click "Load Sequence"-> "Close Window."
5. To see real time current and stimulation, select "File"->"Live Data Monitor". A new window will open.

- In the new Live DataWindow, format screen for testing by using the autoscale function, or manually enter the maximum and minimum y-values displayed on the screen.

3. Animal Set-up

NOTE: All force measurements are those of an 11 week-old Lewis rat. There is a linear correlation between muscle mass and force production (in Newtons). Therefore, as the age of the rat increases, the force values produced by the leg should increase as well.

- Ensure that the animal is in the proper plane of anesthesia before removing it from the anesthesia chamber. Completely remove all hair on the lateral side between the ankle and pelvis of the experimental leg using an electric hair clipper.
NOTE: The proper plane of anesthesia is achieved when the animal is non-responsive to a toe pinch. It is necessary to follow the guidelines put forth by each institution's Animal Care and Use Committee.
- Place the animal in the supine position, ensuring the nose of the animal is securely in the anesthesia nose cone so it remains at the sufficient depth of anesthesia.
- Regulate the position of the pedal apparatus by three independent knobs (**Figure 2**). Using the knobs (A and B) to adjust the foot pedal, place the pedal apparatus at its far left and lowest position, respectively. This will enable the correct positioning of the animal's foot while leaving room for later manipulations. At this position, use the knob on the left of the track to move the apparatus either toward or further away from the experimenter so that the animal leg lies in a straight plane.
- Clean the leg with three changes of iodine and alcohol. The iodine should remain on the leg for 30 sec.
- Adjust the animal or platform (**Figure 2A, D**) so that the extended leg ensures complete contact between the sole of the foot and the foot pedal.
- Using medical tape, secure the foot of the animal against the foot plate (**Figure 2D**). It is crucial that the heel is flush against the bottom of the pedal and the entire foot is flat and will not dislodge from the plate during testing.
- Locate the clamping mechanism to stabilize the leg. Push the stabilizing pin in far enough to reduce movement of the leg and lock it in place by turning the Allen wrench.
- At this position, use the knob C to move the apparatus either toward or away from the experimenter so that the ankle, tibia, and femur lie in a straight line (**Figure 2C**). Ensure that the leg is parallel with the foot pedal. Make adjustments on the course and fine knobs found on the back of the apparatus, to slowly move the ankle so the foot and tibia are at a 90° position.
- Continue to move the leg so the femur and Tibia are at a 90-degree perpendicular angle (**Figure 2B**). At this point, the animal is ready for the electrodes.

4. Placement of the Electrodes

- Activate "Instant Stim" by clicking on the orange button labeled "Instant Stim".
- Place both electrodes superficially on the proximal end of the tibialis anterior and move the electrode tips around until spikes are seen on the live monitor. Ideally, the spikes should be around 0.4 N.
NOTE: The electrodes should be placed adjacent and orthogonal to the plane of peroneal nerve, which in turn, runs laterally from the knee and perpendicular to the tibia.
- Insert one needle far enough to pierce dermis, and barely into the muscular layer. Move the other electrode around until spikes are seen on the live monitor around 0.6 N. Insert needles and clamp them into place using a hobby clamp or medical tape.
- Adjust coarse and fine adjustments to find maximal force output.
- On the high-power bi-phase stimulator, there will be two knobs in the center. One is labeled "RANGE" and the other "ADJUST". Turn the "RANGE" knob to desired maximum amperage.
NOTE: The peaks will slowly increase in magnitude, and the maximum amperage is determined as the level at which three consecutive stimulations result in identical contractile responses. Resist turning the amperage higher than necessary; the maximum amperage will stimulate the entire muscle to contract, but any higher current will result in the recruitment of neighboring muscles and potentially antagonists as well.
- Turn the "ADJUST" knob to set the percentage of the "RANGE" that will be used to stimulate the muscle. At this point, force should read around 1.0 N. This may require an increase or decrease in current.
- Recheck the electrodes to make sure that they are secure. Stop Instant Stim.
- On the "Live Data" window, click "Start Sequence."
- Continue to monitor the curves by going back to the Control Screen, and clicking the "Analysis" button located above the orange "Instant Stim" button. The tetanic curve should begin to take shape around the 60 Hz stimulation.

5. Finishing Stimulation and Clean Up

- After the sequence is finished, remove electrodes and wipe clean with 70% alcohol. Place the electrodes in the covers.
- Unfasten the knee clamp and turn off anesthesia. Remove the animal from the anesthesia gas and place the animal in the prone position, still on the heating pad. Maintain the rat on 100% O₂ for a few minutes after the isoflurane gas has been turned off to keep the rat oxygenated. The animal may move initially, but do not return the animal back to the cage until the animal regains consciousness. If muscle soreness is noticed upon recovery, a dose of NSAID should be given as specified by your animal care committee.
- Turn off all of the equipment listed in step 1.2, close the software, and continue to data analysis.
- Wipe down the platform and foot pedal.

6. Data Analysis

NOTE: Data analysis is performed to fit a sequence designed by this lab and according to lab protocols. Analysis values, data points of importance, and other aspects of the procedure will change depending on the intent of the user.

1. Open the data analysis software.
2. Click on the High Throughput menu to enable analysis of multiple data files (samples) at a time. Select "Force Frequency" Analysis.
3. Click on the "Pick Files" button and open as many saved data files as desired.
4. Select "Manual" in the Cursor Placement Method box.
NOTE: This will allow the user to analyze all of the data within a desired timestamp, as opposed to the program automatically select the analysis location.
5. Change the End Cursor timestamp value to 2. Click the "Analyze" button (**Figure 1D**).
6. To save the table and analyze the data using a spreadsheet, click on the "Save Table to ACSII button. This will save the file, and it can be opened with a spreadsheet at a later time.
7. Open the saved data file in spreadsheet.
8. Create an additional column labeled "Absolute Maximum", and determine the difference between the baseline and the maximum values for each sample. This will provide the total maximum force produced at each frequency.
9. To determine torque, multiply each force value by the length of the lever arm.
NOTE: In this case, that would be represented by the foot length of the animal. This protocol uses the average experimentally determined value of 30 mm. The user has now determined the values for the maximum torque produced at each frequency.
10. Graph these values as a torque frequency curve, or, the maximum torque produced by the animal across all stimulation frequencies.
NOTE: This can be identified and used as a single point of comparison between samples.

Representative Results

The tetanic curve can be used to distinguish optimal results from sub-optimal results. This curve usually starts to form at a frequency of 60 Hz. The key factor to obtaining good results is the ability to stimulate the muscle so that it produces its maximal force and maintains that force during tetanus. The ideal curve should have an uninterrupted, sharp, vertical upswing at the time of stimulation, followed by a flat plateau phase with minimal oscillations, and an uninterrupted, sharp vertical decrease period at termination of stimulation (**Figure 4**). Deviations from the ideal curve are indications that the muscle is fatigued (**Figure 5D**) or that the muscle is not being properly stimulated to produce maximal force (**Figure 5B-C**). The latter generally results from incorrect electrode placement leading to failure of maximal recruitment of muscle fibers during stimulation. A distinguishing feature that allows the researcher to determine if a non-ideal curve is the result of incorrect electrode placement or pathological changes to the muscle is whether or not the tetanic curve is complete (fused) or incomplete (unfused). An unfused, incomplete tetanic curve indicates that the electrodes are misplaced, resulting in the muscle not experiencing a maximal contraction. An example of a pathological change in the muscle can be observed as decreased maximal contraction as compared to the control, or a contractile response that more rapidly fatigues.

The three different types of peaks obtained over the course of this procedure represent different electrode and leg positions and can be seen in **Figure 3**. The first peaks will be around 0.4N and occur when the correct electrode placement is determined superficially on the skin (**Figure 3A**). The second set of peaks has higher amplitude, usually around 0.5-0.6N (**Figure 3B**) and occur when the electrodes pierce through the dermis. After these are obtained, the leg and foot are adjusted to maximize force production, which is achieved when the peak amplitude increases to approximately 1N or greater (**Figure 3C**). At this point, Instant Stim can be turned off and the sequence may begin. These guidelines ensure accurate and reproducible results and are key checkpoints throughout the protocol.

The final results can be represented in different ways depending on the information that the user extracted from the force test and the experimental design. In this protocol, the maximum force is measured across all of the frequencies of stimulation, however other data points may be important for a particular researcher or application. One example is the frequency of stimulation at which the tetanic curve begins to take shape. The data can be compared to other results obtained from a previous or later experiment on the same animal, or for comparisons between different treatment groups. Force production can be normalized by body mass to calculate isometric force and provide a more unbiased assessment of the impact of age on the maximal contraction observed. Although animals of differing body weight and age will produce various maximum forces, the shape of the tetanic curve should be consistent between all groups when the procedure is performed correctly.

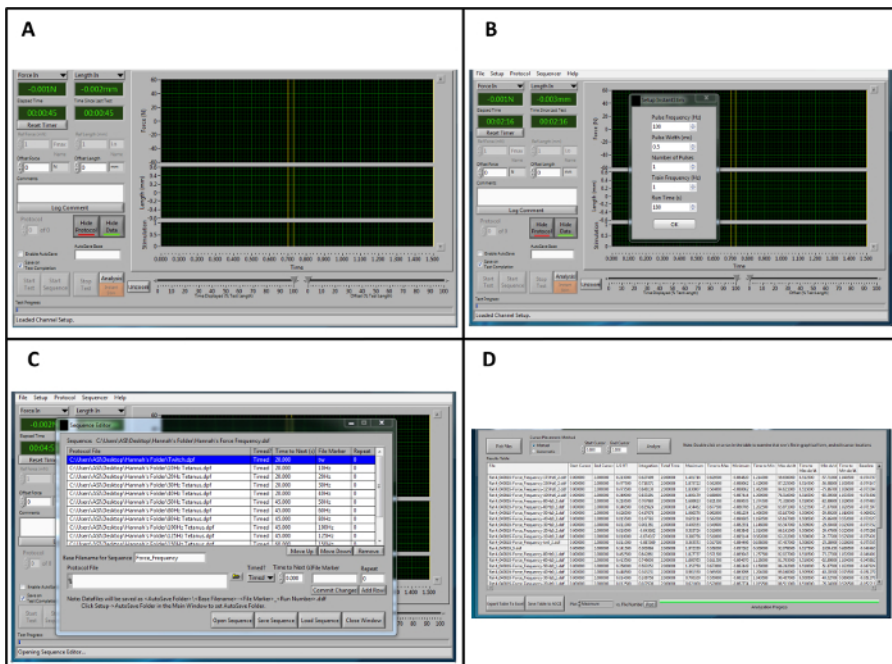


Figure 1: Overview of the Lever system Control and Data Analysis Software for Analysis. (A) Overview of the control software when opening the program. (B) Parameters for "Instant Stim." (C) Example sequence for force-frequency stimulation. (D) Representative data from a high throughput force frequency analysis in the analysis software. It should be noted that the example sequence and data analysis procedure is specific to this protocol and does not represent the full range of sequences and outputs that are provided by this software. [Please click here to view a larger version of this figure.](#)

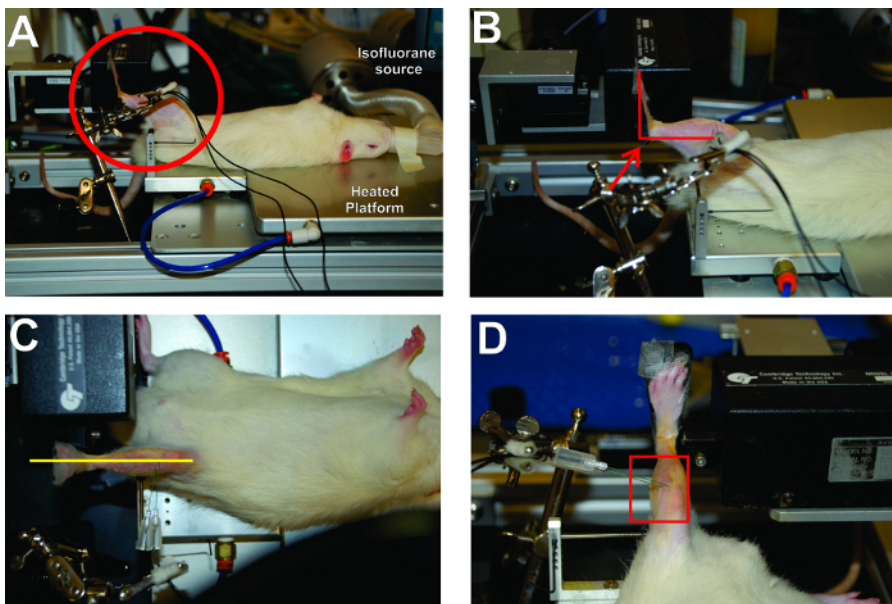


Figure 2: Critical Aspects for Positioning of the Rat and Placement of the Foot in the Apparatus. (A) The rat is in a supine position with the left foot securely attached to the footplate. The right angles made by the foot, leg, and thigh are circled. (B) The right angle created by the ankle is highlighted. (C) The leg should be aligned in a straight plane from foot to body. (D) The electrode placement is parallel and orthogonal to the plane of the peroneal nerve. [Please click here to view a larger version of this figure.](#)

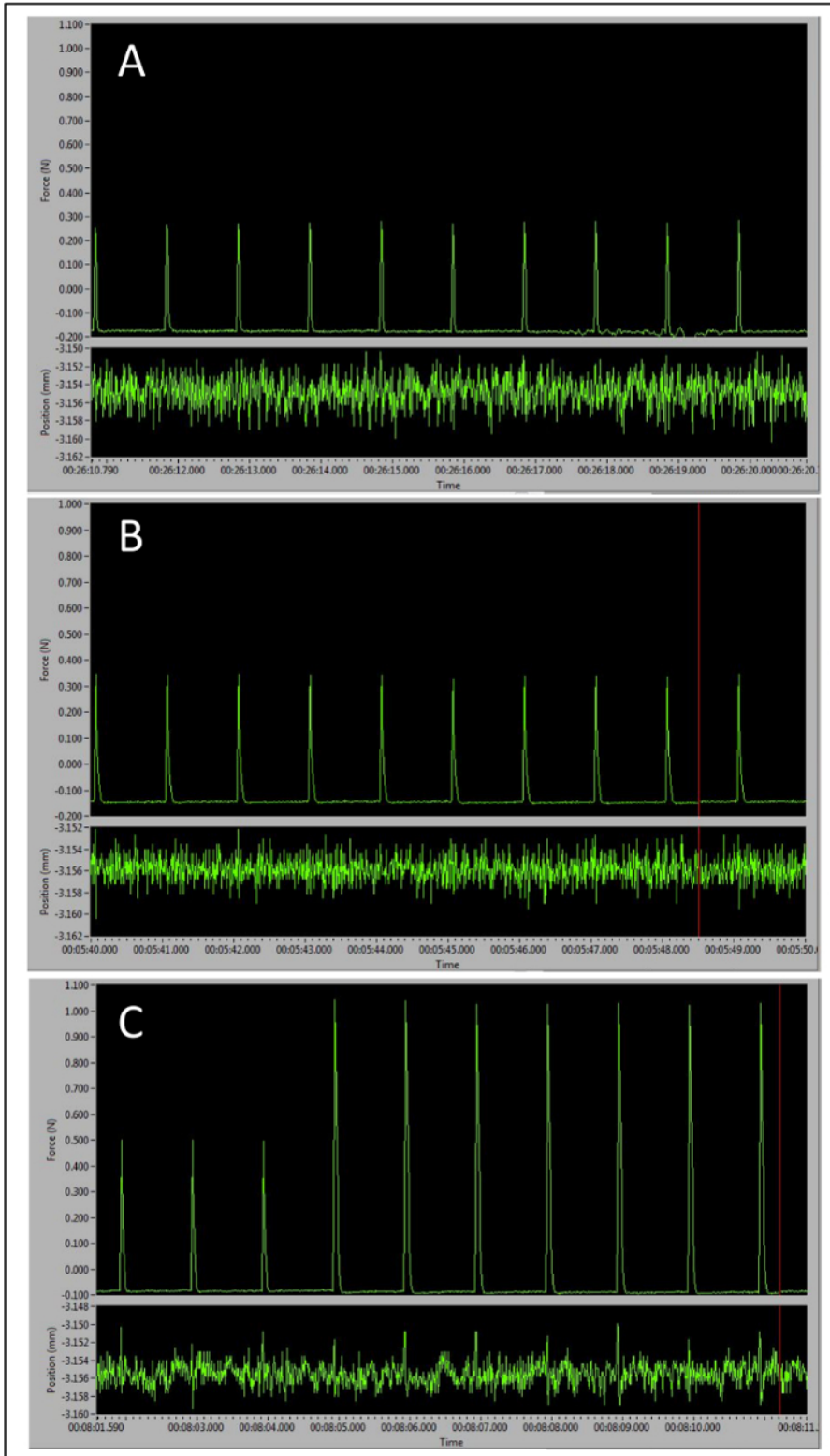


Figure 3: Representative Peaks Demonstrating the Importance of Correct Electrode Placement to Maximal Force Production. (A) Baseline peak tetanic responses observed with electrodes placed too superficially. **(B)** Larger peaks with electrodes inserted in the correct place. **(C)** Transition from larger peaks signaling correct electrode placement to optimal pre-sequence peak amplitude as the leg and foot positions are optimally adjusted. [Please click here to view a larger version of this figure.](#)

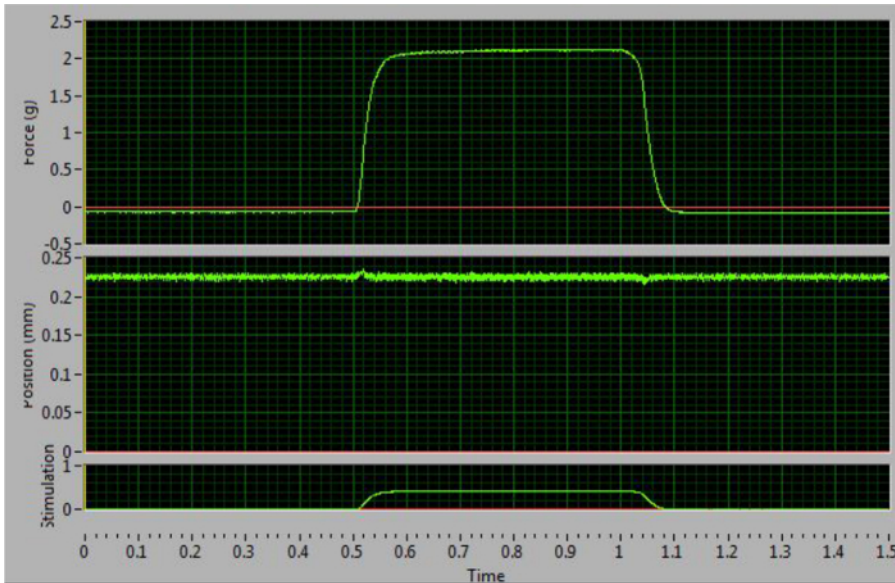


Figure 4: Optimal Tetanic Curve at 100 Hz. This curve increases and decreases sharply and has a flat plateau phase. This example indicates correct electrode placement and maximal force stimulation. [Please click here to view a larger version of this figure.](#)

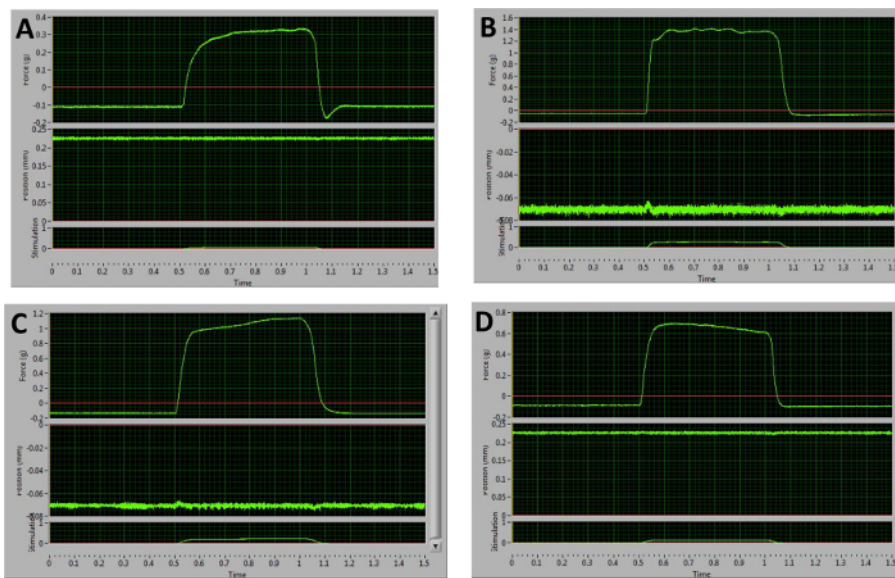


Figure 5: Representative Examples of Sub-optimal Tetanic Curves Obtained at 100 Hz. (A) Following relaxation, this curve dips below the baseline. This is indicative of stimulation of antagonists. (B-D) These graphs are the result of improper electrode placement and unequal recruitment of muscle fibers. The plateau phases demonstrate large oscillations (B), an upward slope (C), or a downward slope (D). [Please click here to view a larger version of this figure.](#)

Discussion

This protocol demonstrates a relatively simple method for performing *in vivo* muscle function testing on the anterior crural compartment of the rat hindlimb. Other forms of muscle function testing, including *ex vivo* and *in situ* protocols, can also provide important information about muscle physiology. However, the significance of *in vivo* function testing lies in its noninvasive nature, and the fact that it most accurately recapitulates endogenous mechanisms of muscle stimulation. For both *ex vivo* and *in situ* testing, the tendon and/or muscle are exposed, and therefore, must be kept moist or submerged^{41,42}. *In vivo* testing removes confounding variables of trauma and inflammation that may be caused by the surgical procedures required for *in situ* muscle function testing; this is especially important if the goal of the experiment is to investigate inflammatory and cellular processes⁴³. Moreover, *in vivo* testing requires little surgical skill as the muscle is not isolated from its surroundings and does not require precise knots to reduce muscle/tendon slippage (as is the case for *in situ* or *ex vivo* testing)⁴¹. In addition, with sufficient practice, the speed of correct electrode placement and the ability to quickly make adjustments to achieve maximal force production of the muscle will ensure that protocol completion is rapid and reproducible- both within animals and across different users of the same equipment³⁹. It is beneficial to begin with an assessment of the entire anterior crural component as illustrated, prior to excision of the less accessible synergistic muscles (EDL and HL) for more direct investigation of the TA muscle. Using this approach, one can rather quickly achieve mastery of the technique. While the procedure described herein demonstrates and highlights the utility of a force frequency protocol to induce tetanus and determine the maximum

force produced by a muscle, users should determine the type(s) of functional testing that would best inform their specific experiment(s) and research goals.

There are several critical steps that should be carefully performed in order to ensure optimal and reproducible experimental outcomes, that is, consistent maximal force production by the muscle to a variety of stimulation parameters. Several of the key features are outlined in **Figure 2**. However, proper placement and stability of the stimulating electrode is an absolute prerequisite for reproducible maximal stimulation of the peroneal nerve. In this regard, the electrodes should be placed superficially. That is, if the electrode placement is too deep, one risks direct electrical stimulation of antagonist muscles, thus diminishing the magnitude of the observed contractile response of the anterior crural compartment. Further, the two electrodes should be placed in as close proximity to each other as feasible to reduce the electrical resistance of the surrounding skin and connective tissue. In general, electrode positioning close to the knee and medial to the leg directly tracing the edge of the tibialis anterior to where it meets the gastrocnemius often yields adequate force production. This also ensures that the electrodes are placed adjacent and orthogonal to the plane of the peroneal nerve, which in turn, runs perpendicular to the tibia and laterally down the leg from the knee. However, the natural variability in anatomy between animals requires constant vigilance to ensure that electrode placement is optimized on case-by-case basis. As such, there is a certain level of trial and error associated with electrode placement that is significantly diminished by the experience of the user. The number of times the electrodes pierce the skin should be minimized to reduce swelling and inflammation, which decreases measured force production. This is dependent on where the needles are initially placed, but it is recommended to move the needles two times or less particularly in the area around the kneecap. Finally, once the electrodes are placed in the leg of the animal, minor adjustments can be made to the positioning of the leg and the current delivered through the electrodes. This should be done while simultaneously monitoring the force produced from a single twitch. In addition to electrode placement, adjustments can also be made to the voltage delivered across the electrodes. However, in the setup described here, it is important to use caution when increasing the voltage as a way to increase force output because the increased voltage will stimulate the nerves that innervate antagonist muscles.

There are three key technical concerns that must be monitored to ensure that the electrode placement remains optimal. First, the foot of the anesthetized animal must be securely anchored to the foot pedal apparatus, which measures the muscle force production (**Figure 2**). If the foot is not securely anchored, the true force produced by the muscle may be incompletely translated to the force transducer. Unstable foot fixation also introduces the risk of losing the optimal placement of the electrodes as motion beyond normal muscle contraction (*i.e.* the foot moving away from the footplate) can cause displacement of the electrodes from their superficial position or dislodge them completely. Either scenario will decrease the measured force. Second, the animal's body should be completely supine and aligned in a straight plane (**Figure 2**). Correct positioning of the animal's body prevents slight movements of the leg due to respiration, and also minimizes twisting of the leg and pelvis, enabling better placement and continuous contact of the stimulating electrodes. Third, correct positioning and anchoring of the knee is critical to ensure that the leg remains steady, and thus, helps stabilize the optimal placement of the stimulating electrodes to permit consistent activation of the peroneal nerve.

There are a few additional points that should be emphasized. First, the commercial muscle lever system is designed to perform testing on the left leg, however the setup may be modified to perform testing on the right leg as well. Second, muscle lever systems may be chosen based on the size of the animal, so users should ensure that the platform used is adequate to measure and support the force produced by the animal model of choice. Testable muscles for the equipment platform are limited to those that induce plantar extension or dorsiflexion of the foot. Third, it should again be emphasized that electrode placement can be challenging and requires patience and practice to master the technique. Electrodes also become dull quickly with regular use, so it is helpful to have several spare sets for once it becomes difficult to prick the skin superficially. Third, the protocol described in this report utilizes specific stimulation sequences and data analysis procedures. The muscle lever system control software and data analysis software and the data it provides can answer many other experimental questions and therefore, its utility extends beyond what is outlined herein. As such, users are encouraged to explore beyond the limits of the software protocol(s) presented in this paper. Despite these minor limitations, *in vivo* muscle function testing is a powerful approach to determine the health and contractile ability of skeletal muscle because it is minimally invasive and can be performed on multiple occasions, over an extended time frame, on the same animal. In short, this type of serviceable utility makes the system particularly adept at testing the effects of novel therapies for skeletal muscle injury or disease in the rat hindlimb.

Disclosures

The authors have nothing to disclose.

Acknowledgements

The authors would like to thank Dr. Hannah Baker for her extensive work in optimizing this procedure.

References

1. Jarvinen, T. A., Jarvinen, T. L., Kaariainen, M., Kalimo, H., & Jarvinen, M. Muscle injuries: biology and treatment. *Am J Sports Med.* **33**, 745-764 (2005).
2. Ciciliot, S., & Schiaffino, S. Regeneration of mammalian skeletal muscle. Basic mechanisms and clinical implications. *Curr Pharm Des.* **16**, 906-914 (2010).
3. Lin Shiau, S. Y., Huang, M. C., & Lee, C. Y. Mechanism of action of cobra cardiotoxin in the skeletal muscle. *J Pharmacol Exp Ther.* **196**, 758-770 (1976).
4. Lepper, C., Partridge, T. A., & Fan, C. M. An absolute requirement for Pax7-positive satellite cells in acute injury-induced skeletal muscle regeneration. *Development.* **138**, 3639-3646 (2011).
5. Charge, S. B., & Rudnicki, M. A. Cellular and molecular regulation of muscle regeneration. *Physiol Rev.* **84**, 209-238 (2004).
6. Couteaux, R., Mira, J. C., & d'Albis, A. Regeneration of muscles after cardiotoxin injury. I. Cytological aspects. *Biol Cell.* **62**, 171-182 (1988).

7. d'Albis, A., Couteaux, R., Janmot, C., Roulet, A., & Mira, J. C. Regeneration after cardiotoxin injury of innervated and denervated slow and fast muscles of mammals. Myosin isoform analysis. *Eur J Biochem.* **174**, 103-110 (1988).
8. Reali, M., Serafim, F. G., da Cruz-Hofling, M. A., & Fontana, M. D. Neurotoxic and myotoxic actions of *Naja naja kaouthia* venom on skeletal muscle in vitro. *Toxicon.* **41**, 657-665 (2003).
9. Sambasivan, R., & Tajbakhsh, S. Adult skeletal muscle stem cells. *Results Probl Cell Differ.* **56**, 191-213 (2015).
10. Le Grand, F., & Rudnicki, M. A. Skeletal muscle satellite cells and adult myogenesis. *Curr Opin Cell Biol.* **19**, 628-633 (2007).
11. Mauro, A. Satellite cell of skeletal muscle fibers. *J Biophys Biochem Cytol.* **9**, 493-495 (1961).
12. Brack, A. S., & Rando, T. A. Tissue-specific stem cells: lessons from the skeletal muscle satellite cell. *Cell Stem Cell.* **10**, 504-514 (2012).
13. Sambasivan, R. *et al.* Pax7-expressing satellite cells are indispensable for adult skeletal muscle regeneration. *Development.* **138**, 3647-3656 (2011).
14. Lees, S. J., Rathbone, C. R., & Booth, F. W. Age-associated decrease in muscle precursor cell differentiation. *Am J Physiol Cell Physiol.* **290**, C609-615 (2006).
15. Rotter, R. *et al.* Erythropoietin improves functional and histological recovery of traumatized skeletal muscle tissue. *J Orthop Res.* **26**, 1618-1626 (2008).
16. Rathbone, C. R., Wenke, J. C., Warren, G. L., & Armstrong, R. B. Importance of satellite cells in the strength recovery after eccentric contraction-induced muscle injury. *Am J Physiol Regul Integr Comp Physiol.* **285**, R1490-1495 (2003).
17. Bassel-Duby, R., & Olson, E. N. Signaling pathways in skeletal muscle remodeling. *Annu Rev Biochem.* **75**, 19-37 (2006).
18. Bentzinger, C. F., Wang, Y. X., & Rudnicki, M. A. Building muscle: molecular regulation of myogenesis. *Cold Spring Harb Perspect Biol.* **4** (2012).
19. von Maltzahn, J., Chang, N. C., Bentzinger, C. F., & Rudnicki, M. A. Wnt signaling in myogenesis. *Trends Cell Biol.* **22**, 602-609 (2012).
20. Collu, G. M., Hidalgo-Sastre, A., & Brennan, K. Wnt-Notch signalling crosstalk in development and disease. *CMLS.* **71**, 3553-3567 (2014).
21. Bjornson, C. R. *et al.* Notch signaling is necessary to maintain quiescence in adult muscle stem cells. *Stem Cells.* **30**, 232-242 (2012).
22. Vignaud, A., Hourde, C., Butler-Browne, G., & Ferry, A. Differential recovery of neuromuscular function after nerve/muscle injury induced by crude venom from *Notechis scutatus*, cardiotoxin from *Naja atra* and bupivacaine treatments in mice. *Neurosci Res.* **58**, 317-323 (2007).
23. Grogan, B. F., Hsu, J. R., & Skeletal Trauma Research, C. Volumetric muscle loss. *J Am Acad Orthop Surg.* **19 Suppl 1**, S35-37 (2011).
24. Sicari, B. M. *et al.* A murine model of volumetric muscle loss and a regenerative medicine approach for tissue replacement. *Tissue Eng Part A.* **18**, 1941-1948 (2012).
25. Wu, X., Corona, B. T., Chen, X., & Walters, T. J. A standardized rat model of volumetric muscle loss injury for the development of tissue engineering therapies. *Biores Open Access.* **1**, 280-290 (2012).
26. Armstrong, R. B., & Phelps, R. O. Muscle fiber type composition of the rat hindlimb. *Am J Anat.* **171**, 259-272 (1984).
27. Yeh, L. S., Gregory, C. R., Theriault, B. R., Hou, S. M., & Lecouter, R. A. A functional model for whole limb transplantation in the rat. *Plast Reconstr Surg.* **105**, 1704-1711 (2000).
28. Lin, J. B. *et al.* Imaging of small animal peripheral artery disease models: recent advancements and translational potential. *Int J Mol Sci.* **16**, 11131-11177 (2015).
29. Larcher, T. *et al.* Characterization of dystrophin deficient rats: a new model for Duchenne muscular dystrophy. *PLoS one.* **9**, e110371 (2014).
30. Warren, G. L., Stallone, J. L., Allen, M. R., & Bloomfield, S. A. Functional recovery of the plantarflexor muscle group after hindlimb unloading in the rat. *Eur J Appl Physiol.* **93**, 130-138 (2004).
31. Muller-Delp, J. M., Spier, S. A., Ramsey, M. W., & Delp, M. D. Aging impairs endothelium-dependent vasodilation in rat skeletal muscle arterioles. *Am J Physiol Heart Circ Physiol.* **283**, H1662-1672 (2002).
32. Liu, M., Bose, P., Walter, G. A., Thompson, F. J., & Vandenborne, K. A longitudinal study of skeletal muscle following spinal cord injury and locomotor training. *Spinal Cord.* **46**, 488-493 (2008).
33. Yoshida, H. *et al.* A phosphodiesterase 3 inhibitor, K-134, improves hindlimb skeletal muscle circulation in rat models of peripheral arterial disease. *Atherosclerosis.* **221**, 84-90 (2012).
34. Regensteiner, J. G. *et al.* Chronic changes in skeletal muscle histology and function in peripheral arterial disease. *Circulation.* **87**, 413-421 (1993).
35. Park, K. H. *et al.* Ex vivo assessment of contractility, fatigability and alternans in isolated skeletal muscles. *J Vis Exp.* e4198 (2012).
36. MacIntosh, B. R., Esau, S. P., Holash, R. J., & Fletcher, J. R. Procedures for rat in situ skeletal muscle contractile properties. *J Vis Exp.* e3167 (2011).
37. Grassi, B., Gladden, L. B., Samaja, M., Stary, C. M., & Hogan, M. C. Faster adjustment of O₂ delivery does not affect V(O₂) on-kinetics in isolated in situ canine muscle. *J Appl Physiol (1985).* **85**, 1394-1403 (1998).
38. Chiu, C. S. *et al.* Non-invasive muscle contraction assay to study rodent models of sarcopenia. *BMC Musculoskelet Disord.* **12**, 246 (2011).
39. Corona, B. T., Ward, C. L., Baker, H. B., Walters, T. J., & Christ, G. J. Implantation of in vitro tissue engineered muscle repair constructs and bladder acellular matrices partially restore in vivo skeletal muscle function in a rat model of volumetric muscle loss injury. *Tissue Eng Part A.* **20**, 705-715 (2014).
40. Burks, T. N. *et al.* Losartan restores skeletal muscle remodeling and protects against disuse atrophy in sarcopenia. *Sci transl med.* **3**, 82ra37 (2011).
41. Brooks, S. V., Zerba, E., & Faulkner, J. A. Injury to muscle fibres after single stretches of passive and maximally stimulated muscles in mice. *J Physiol.* **488 (Pt 2)**, 459-469 (1995).
42. Machingal, M. A. *et al.* A tissue-engineered muscle repair construct for functional restoration of an irrecoverable muscle injury in a murine model. *Tissue Eng Part A.* **17**, 2291-2303 (2011).
43. Pizza, F. X., Koh, T. J., McGregor, S. J., & Brooks, S. V. Muscle inflammatory cells after passive stretches, isometric contractions, and lengthening contractions. *J Appl Physiol (1985).* **92**, 1873-1878 (2002).